# The temperature dependence of heavy-ion damage in iron: a microstructural transition at elevated temperatures

Zhongwen Yao, Mike Jenkins, Mercedes Hernández-Mayoral, Mark Kirk

# The temperature dependence of heavy-ion damage in iron: a microstructural transition at elevated temperatures

| | |
|---|---|
| Note: The following files were submitted by the author for peer review, but cannot be converted to PDF. You must view these files (e.g. movies) online. | |
| video 1.mov<br>Video 2.mov<br>Video 3.mov<br>Video 4.mov<br>Video 5.mov<br>Video 6.mov | |

# The temperature dependence of heavy-ion damage in iron: a microstructural transition at elevated temperatures

Z. Yao[*], M. L. Jenkins[*1], M. Hernández-Mayoral[**] and M. A. Kirk[***]

[*] Department of Materials, University of Oxford, Parks Rd., OX1 3PH
[**]Division of Materials, CIEMAT Avenida Complutense, 22, 28040-Madrid
[***]Materials Science Division, Argonne National Laboratory, Argonne, IL 60439

[1] Corresponding author: Email: mike.jenkins@materials.ox.ac.uk

1

1
2
3
4
5
6
7
8
9
10
11
12
13
14
15
16
17
18
19
20
21
22
23
24
25
26
27
28
29
30
31
32
33
34
35
36
37
38
39
40
41
42
43
44
45
46
47
48
49
50
51
52
53
54
55
56
57
58
59
60

**Abstract**

We describe a transition in the dislocation microstructure of pure Fe produced by heavy-ion irradiation of thin foils which took place between irradiation temperatures $T_{irr}$ of $300^{\circ}C$ and $500^{\circ}C$. At $T_{irr} \leq 400^{\circ}C$, the microstructure was dominated by round or irregular non-edge dislocation loops of interstitial nature and with Burgers vectors $\mathbf{b} = \frac{1}{2}<111>$, although interstitial $<100>$ loops were also present; at $500^{\circ}C$ only rectilinear pure-edge $<100>$ loops occurred. At intermediate temperatures there was a gradual transition between the two types of microstructure. At temperatures just below $500^{\circ}C$, mobile $\frac{1}{2}<111>$ loops were seen to be subsumed by sessile $<100>$ loops. A possible explanation of these observations is given.

**Deleted:**

**Deleted:** a/2

**Deleted:** a

**Deleted:** square

**Deleted:** a

**Deleted:** a/2

**Deleted:** a

2

### 1. Introduction

It has been long known that the mechanical properties of steels start to degrade at temperatures above about 500°C - a relatively low temperature ($0.42T_m$). According to recent theoretical calculations [1,2], a possible cause of this is an elastic instability, driven by spin fluctuations. This results in a large reduction in the shear stiffness constant $C' = (C_{11} - C_{12})/2$ at the $\alpha \to \gamma$ phase transition temperature of $912^o$C, although effects on mechanical properties are manifest at temperatures well below this. The same theory predicts that dislocation loops with Burgers vector $\mathbf{b} = \langle 100 \rangle$ will become relatively more stable with respect to loops with $\mathbf{b} = \frac{1}{2}\langle 111 \rangle$ with increasing temperature.

In previous papers we have described *in-situ* ion-irradiation experiments which followed the evolution of microstructures in thin foils of pure iron (Fe) and FeCr alloys at irradiation temperatures $T_{irr} \leq 300^o$C [3-5] and at $500^o$C [5]. These experiments provided support for the view that dislocation loops with $\mathbf{b} = \langle 100 \rangle$ increase in stability with temperature. For $T_{irr} \leq 300^o$C, the microstructures both in pure Fe and in FeCr alloys irradiated with 150 keV $Fe^+$ ions were dominated by interstitial loops with Burgers vectors $\mathbf{b} = \frac{1}{2}\langle 111 \rangle$. These loops were frequently round or of irregular shape and had significant shear components, and sometimes coalesced into large finger-shaped loops. However, in the same materials irradiated at 500°C, only rectilinear pure-edge interstitial loops with $\mathbf{b} = \langle 100 \rangle$ loops were present.

In the present paper this transition in microstructures is explored in more detail in pure Fe. All images and videos included in this paper were recorded under weak-beam diffraction conditions [6]. The weak-beam method of transmission electron microscopy has become an indispensable tool in this area of research (for a review giving full experimental details, see ref. [7]).

### 2. Experimental method

The materials were the same as those investigated previously (annealed ultra-high purity polycrystalline Fe and a somewhat less pure Fe single crystal – see ref. [3] for details). Full details of specimen preparation and irradiation in the Argonne-IVEM Tandem Facility have been given in a previous paper [3]. Briefly, specimens were electro-polished with minimum exposure to air and introduced immediately into an Hitachi H-9000NAR transmission electron microscope interfaced to an ion implanter. They were then irradiated with 150 keV $Fe^+$ self ions at temperatures ranging $400^o$C to 500 °C, with an estimated accuracy of $\pm 10^o$C. We estimate that for this irradiation condition the peak of the damage occurs at a depth of about 28 nm [3]. The regions of foil investigated in the TEM were typically of thickness 30-40 nm, so the damage peak was close to the foil centre. We found in our previous work that in such foils small $\frac{1}{2}\langle 111 \rangle$ dislocation loops were very mobile, and in some foil orientations some of these loops were lost by glide to the foil surfaces under the influence of surface image forces [3-5]. For this reason the single-crystal Fe used in some of the present experiments was spark-cut into slices parallel to the (110) plane in order to obtain TEM specimens with a [110] foil normal. In

**Deleted:** a

**Deleted:** a/2

**Deleted:** a

**Deleted:** a/2

**Deleted:** a

**Deleted:** )

**Deleted:** The single-crystal Fe was spark-cut into slices parallel to the (110) plane in order to obtain TEM specimens with a [110] foil normal for reasons given in section 3.2.

3

foils of this orientation some loop variants have their Burgers vectors in or close to the foil plane, and so cannot easily be lost by glide (see section 3.3 for details).

The evolution of radiation damage was followed by dynamic TEM observations under weak-beam diffraction conditions to doses $\leq 2 \times 10^{19}$ ions m$^{-2}$ (~13 dpa). In most of the present experiments irradiations were terminated at a dose of 2 or $3 \times 10^{18}$ ions m$^{-2}$ (~1.3-2 dpa). Irradiations were paused from time to time to allow detailed characterization of microstructures using standard diffraction-contrast techniques [7]. Similar detailed characterization was performed at the end of the irradiation after specimens had cooled to room temperature.

### 3. Results

### *3.1*     *$T_{irr} = 400^oC$*

At doses $<10^{18}$ ions m$^{-2}$, the initial damage microstructure was similar to that seen in previous experiments at 300$^o$C. Small dislocation loops, visible as white dots of diameter less than about 5 nm in weak-beam images, appeared within a timescale of a few video frames. Most of these loops were extremely mobile, making large and frequent "hops" in <111> directions, consistent with ½<111> Burgers vectors. The frequencies and amplitudes of hops were much larger than those seen in the same material at 300°C [3] or in the 1-D diffusion of loops seen in similar material under electron irradiation at temperatures < 400$^o$C [8]. As the irradiation progressed, loops were seen to interact elastically, making coordinated hops and occasionally coalescing into larger loops.  This behaviour is illustrated in video 1, which shows damage development under ion irradiation over a dose range 0 - $5 \times 10^{17}$ ions m$^{-2}$. The coalescence after irradiation of a string of three ½<111> loops into a larger, but still mobile ½<111> loop which then rotates on its glide cylinder is shown in video 2, with stills from this video in figure 1. By a dose of $2 \times 10^{18}$ ions m$^{-2}$ (~1.3 dpa), elastic interactions led to the formation of chains of large (30-50 nm), round loops in thicker areas, reminiscent of those seen at lower irradiation temperatures [3-5] but on a larger scale. The formation of loop chains under irradiation may be viewed dynamically in video 3.

In video 3, it may be seen that a number of loops appeared more gradually and were immobile, and it was surmised that these had <100> Burgers vectors. A post-irradiation Burgers vector analysis was carried out at the final dose of $2 \times 10^{18}$ ions$^{-2}$, and selected micrographs from this experiment are shown in figure 2. The analysis confirmed that both ½<111> and <100> loops had formed. Large (30-50 nm) loops had Burgers vectors $\mathbf{b} = \frac{1}{2}[1\bar{1}1]$ or $\mathbf{b} = \frac{1}{2}[11\bar{1}]$ (and so were out of contrast in figure 2d) or $\mathbf{b} = [001]$ (and so were out of contrast in figure 2a). Interestingly, no large loops of the other variants were seen in this area. Small (~ 10 nm) loops of each type and variant were also present.  The number density of <100> loops was larger than that of ½<111> loops, but on average they were much smaller, so that a majority of point defects was contained in ½<111> loops. This will be quantified and discussed later. Stereo experiments showed that large loops were localized towards the foil centre, whilst smaller loops were distributed throughout the foil, regardless of their Burgers vectors. This may be seen in

4

video 4, which shows a tilt series constructed using EM3D tomography software from a set of 7 stereo images taken over a tilt range of ~35° with **g** = 002.

By inspection of figure 2 it may be seen that the large [001] loops are of pure-edge type. The foil normal in this micrograph is [100] and edge-on loops with **b** = [001] are seen to lie perpendicular to the diffraction vector **g** = $00\bar{2}$ in figure 2c. Similar pure-edge <100> loops were found in our previous work at $T_{irr} = 500°C$, where their nature was determined to be interstitial [5]. Micrographs taken at other orientations showed that <100> loops larger than about 20nm were rectilinear with edges along <100> directions. Smaller ones looked more rounded. The detailed shape of loops is discussed in a separate paper [9].

The ½<111> loops are non-edge. A full Burgers vector analysis (carried out using the reflections available at both the [110] and [100] poles) showed that the predominant Burgers vector of the large loops in the area of foil shown in figure 3a was ½[$\bar{1}$11]. The habit plane of these loops was found by tilting the foil from pole [110] → [310] → [100], whilst maintaining the same weak-beam diffraction condition with **g** = 002. The loops appear edge-on at the [310] pole, imaging as lines lying perpendicular to the [$\bar{1}$32] direction (figure 3a). They therefore lie on or close to the ($\bar{1}$32) plane, so that the angle between the loop normal **n** and **b** is about 22°. Figures 3b and 3c show experimental images of two loops recorded close to the [110] and [310] poles respectively. Image simulations using the program TEMACI [10] for circular loops with **b** = ½[$\bar{1}$11] with a ($\bar{1}$32) habit plane are inset at the lower left of each figure. The good match between experimental and simulated images confirms our interpretation. In our previous experiments in UHP-Fe at 300°C the large ½<111> "finger" loops which formed at high doses were also found to have significant shear components and were also found to be interstitial [4].

### 3.2 $T_{irr} = 450°C$

In an experiment carried out at $T_{irr} = 450°C$ on an UHP Fe foil oriented about 20° from [111], early stages in damage development were similar to those seen at 400°C, except that larger-scale microstructures appeared more slowly. Small loops were seen early in the irradiation, and were extremely mobile, and were frequently lost from the foil. As the dose increased, again chains of loops formed, interacting elastically. By a dose of 3 x $10^{18}$ ions m$^{-2}$, long lines of large ½<111> loops had formed in thicker regions, all with the same Burgers vector, and looking similar to the microstructure examined in detail at 400°C (figure 4a). In an adjacent grain tilted close to [100], regions were found where large loops of both <100> and ½<111> types were present (figure 4b), although <100> loops were in a preponderance. In other regions of this grain large numbers of edge-on <100> loops were visible (figure 4c). The absence of ½<111> loops in figure 4c may well be a contrast effect: the large loops in figure 4b are visible in **g** = $01\bar{1}$ and so have either **b** = ½[$1\bar{1}1$] or **b** = ½[$11\bar{1}$], but loops with these Burgers vectors would be out of contrast in figure 4c which was taken in **g** = 011. The average sizes of <100> loops were significantly larger than at 400°C, and a majority of point-defects was now contained in

Deleted: a
Deleted: a
Deleted: a
Deleted: a
Deleted: a/2
Deleted: a/2
Deleted: a/2
Deleted: a/2
Deleted: a/2
Deleted: a
Deleted: a/2
Deleted: a
Deleted: a
Deleted: a/2
Deleted: a/2
Deleted: a/2
Deleted: a

5

such loops, see below. This temperature seems to mark a transition from a mostly ½<111> microstructure to a microstructure dominated by <100> loops.

### *3.3    $T_{irr} = 460^oC - 500^oC$*

At 500°C, we found in our previous work that only <100> loops formed in [100] foils [5]. These loops appeared slowly over several minutes, and were immobile. Figure 5a shows the microstructure at a dose of $3 \times 10^{18}$ ions m$^{-2}$, where loops of sizes up to about 50 nm were present but well separated.  As these loops grew under continuing irradiation, they coalesced with neighbouring loops with the same Burgers vector until they impinged on loops of the other variants, forming the microstructure seen in figure 5b. In this figure, loops belonging to all three <100> variants can be seen. Two variants, with **b** = [001] and **b** = [010], appear edge-on, forming a quasi-regular ladder-like structure. Loops of the third variant, with **b** = [100], lie in the plane of the foil and are faintly visible in residual **g.b** × **u** contrast. Occasionally during irradiation loops with this Burgers vector were suddenly lost from the foil by glide, see video 5, demonstrating that <100> loops are not intrinsically sessile.

In foils with normal [100], all variants of ½<111> loops have a component of Burgers vector pointing towards the surface. Since ½<111> loops are highly mobile at 500°C, the possibility exists that such loops do form, but are lost by glide to the surface before they are seen. Total loss of ½<111> loops in (100) foils is known to occur in ion-irradiated Mo [11].  In order to exclude this possibility, the following experiments were carried out in single-crystal foils with orientation close to [110]. In such foils, loops with **b** = ½[$\bar{1}$11] and **b** = ½[1$\bar{1}$1] have little or no component of Burgers vector towards the surface, and so cannot easily be lost by glide.

First a foil was irradiated to a moderate dose ($1 \times 10^{18}$ m$^{-2}$) at 500°C. Sessile loops with **b** = <100> were seen to form, but no loops with **b** = ½<111> loops were found[2]. A further irradiation of the same foil was then performed at 482°C. A few small ½<111> loops were produced in the field of view of the CCD camera. All remained in the foil and hopped along <111> directions in the plane of the foil. Soon after irradiation, none of these ½<111> loops could be found. It was not clear by which mechanism they had disappeared.

A second foil was irradiated at 465°C. Video 6 shows this specimen under ion irradiation, and figure 6 shows a series of stills from this video. The video shows directly the fate of ½<111> loops at elevated temperatures. In the area of observation are some easily-recognized, large, sessile, near edge-on <100> loops and two small (~ 5 nm) ½<111> loops, located on either side of a larger (~ 50 nm) <100> loop (arrowed in figure 6). At first, the two ½<111> loops hopped parallel to their Burgers vector. Their glide cylinders did not intersect the <100> loop. However, within a minute both ½<111> loops had moved towards the <100> loop, this motion involving sideways steps perpendicular to their glide cylinders. On reaching the <100> loop they were subsumed, causing the

---

[2] We have recently found the same result in a [110] Fe-C alloy irradiated at 500°C under the same conditions.

6

$\langle 100 \rangle$ loop to grow.  The increase in size of the $\langle 100 \rangle$ loop indicates that the two $\frac{1}{2}\langle 111 \rangle$ loops which it had absorbed had the same nature as the $\langle 100 \rangle$ loop itself, i.e. all were interstitial.

### 4.  Discussion

The occurrence of $\langle 100 \rangle$ loops in Fe irradiated at high temperature has been known since the pioneering work of Masters [12], who carried out thin-foil irradiation experiments similar to our own. Masters found exclusively $\langle 100 \rangle$ loops of interstitial nature in pure Fe irradiated with 150keV $Fe^+$ ions at 550°C.  Subsequently $\langle 100 \rangle$ loops, or a mixture of $\langle 100 \rangle$ and $\frac{1}{2}\langle 111 \rangle$ loops, have been found in many other elevated-temperature experiments in ferritic materials. These include, for example, experiments by Konobeev *et al* [13] who found $\langle 100 \rangle$ interstitial loops (as well as voids) in Fe and Fe 0-18%Cr irradiated with fast neutrons to doses up to 25.8 dpa at 400°C. As a further example, Gelles [14] also found that $\langle 100 \rangle$ loops predominated in Fe3%Cr alloys irradiated with neutrons to ~ 20dpa at temperatures between 400°C and 450°C, although a mixture of the two loop types was found in higher Cr alloys. In our own recent experiments in Fe irradiated in the bulk with 0.5-3 MeV $Fe^+$ ions to ~ 10 dpa at 500°C, we also found almost exclusively interstitial $\langle 100 \rangle$ loops, whilst at 300°C a mixture of $\langle 100 \rangle$ and $\frac{1}{2}\langle 111 \rangle$ loops was present. In FeCr alloys, however, both loop types were present at 500°C [15]. In these and other experiments there does seem a clear pattern for $\langle 100 \rangle$ loops to predominate in pure Fe at irradiation temperatures $T_{irr} \ge 400$°C. In contrast, in Fe irradiated at 60°C with neutrons, only $\frac{1}{2}\langle 111 \rangle$ loops were identified, again of interstitial nature [16]. The only examples we know of $\langle 100 \rangle$ loops in low-temperature irradiations are found in Fe irradiated with $W^+$ ions at room temperature[17] and with high doses of self-ions [18], and in these cases loops were considered to have formed by a process of cascade collapse and the loop nature was *vacancy*.

Our present work has provided further evidence that $\langle 100 \rangle$ loops become increasingly dominant in Fe with increasing irradiation temperature. In figure 7 we have made an attempt to quantify the proportions of interstitials contained in $\langle 100 \rangle$ and $\frac{1}{2}\langle 111 \rangle$ at various temperatures. This figure was constructed by measuring the size distributions and number densities of the two types of loops at different irradiation temperatures. At $T_{irr} = 400$°C, about 80% of loops were of the $\langle 100 \rangle$ type, but their mean size was only about a third that of the $\frac{1}{2}\langle 111 \rangle$ loops, and so the fraction of interstitials contained in loops of the two types was comparable. At $T_{irr} = 450$°C, the majority of interstitials was contained in $\langle 100 \rangle$ loops, but large $\frac{1}{2}\langle 111 \rangle$ round loops were still present in some areas. At $T_{irr} \ge 492$°C, no $\langle 111 \rangle$ loops were seen during ion irradiation, whereas $\langle 100 \rangle$ loops formed and grew. As a rough estimate, the total number of interstitials contained in $\langle 100 \rangle$ loops at 500°C was comparable with the number of interstitials  contained in loops at 300°C, for the same irradiation dose. No correction has been made in figure 7 for loss of mobile $\frac{1}{2}\langle 111 \rangle$ loops to the surface, nor for the effects of foil orientation and thickness, nor for the variability in loop types from area to area. Discussions of these effects may be found in our previous papers [3,5].  Their neglect is likely to lead to an underestimate of the number of interstitials in $\frac{1}{2}\langle 111 \rangle$ loops at all temperatures, but we believe that the trends shown are real.

7

In parallel with our experimental work, Dudarev *et al.* [1,2] developed methods of calculating the self-energy of loops of different Burgers vectors and morphologies as a function of temperature. As mentioned in the introduction, they found that the reduction in the shear stiffness constant C′ with increasing temperature caused a profound effect on the anisotropic elastic self-energies of dislocations in Fe and on the relative stability of $<100>$ and $\frac{1}{2}<111>$ dislocation loops. For example, for loops of perimeter P = 10 nm, hexagonal, prismatic pure-edge dislocation loops with Burgers vector $\frac{1}{2}<111>$ were found to be unconditionally stable at temperatures T < 350°C, whereas square $<100>$ pure-edge loops were unconditionally stable for T > 550°C. In the intermediate temperature region, 350°C < T < 550°C, loops of this size with **b** = $\frac{1}{2}<111>$ and edges along $<\bar{1}10>$ directions were thermodynamically unstable and could lower their free energy either by changing shape (with edges along $<11\bar{2}>$ directions) or by transforming to $<100>$ loops. Dudarev *et al.* [2] argued that in a real situation where loops of various sizes and shapes are present, the boundaries between the different regions of stability would be diffuse, leading to a gradual transition in loop types.

This picture above is clearly in good qualitative accord with our observations. We found that $\frac{1}{2}<111>$ loops were dominant components of the microstructure at temperatures $T_{irr} \le 300°C$, although small $<100>$ loops were present even at room temperature [3,4]. At temperatures $T_{irr} \ge 400°C$, $<100>$ loops became increasingly important components of the microstructure (figure 7). Our observations are therefore compatible with a picture that $<100>$ loops become more energetically favoured with increasing temperature. However the mechanism by which the transition in loop types takes place is still not entirely clear. In particular, the abrupt disappearance of $\frac{1}{2}<111>$ loops at temperatures $T_{irr} >465°C$ was something of a surprise. Unlike Arakawa *et al* [19] we did not see $\frac{1}{2}<111>$ loops transform directly into $<100>$ loops. Small mobile $\frac{1}{2}<111>$ loops were produced at $T_{irr} = 465°C$, but were quickly subsumed by sessile $<100>$ loops. The crabwise motion by which the $\frac{1}{2}<111>$ loops approached the $<100>$ loop (video 6, figure 6) evidently involved self-climb, since the sizes of the $\frac{1}{2}<111>$ loops remained unchanged at the resolution of the CCD camera. Coalescence of interstitial loops by self-climb has been observed previously during an isothermal anneal of ion-implanted $UO_2$ by Turnbull [20]. Turnbull considered two possible driving forces: first the mutual interaction of the loop strain fields, and second the interaction of the strain fields of loops and vacancies. He concluded that in metals both interactions were likely to be important.

Clues to the possible mechanisms underlying our observations may be gleaned from molecular dynamics simulations of displacement cascades in Fe by Bacon and co-workers [21]. In these simulations small, self-interstitial clusters formed at the cascade peripheries at the end of the displacement phase of the cascade in an essentially athermal process, or by short-range diffusion during the thermal-spike phase. Smaller clusters may be considered as bundles of <111> or <100> crowdions. These clusters are very mobile, even at low temperatures, moving by thermally-activated one-dimensional glide along the crowdion direction. Larger clusters of crowdions may be considered as small, but probably sub-microscopic $\frac{1}{2}<111>$ or <100> dislocation loops. We surmise that loops large enough to be seen in the TEM form by the coalescence of such small clusters, and

8

that this process is more likely to occur in the foil interior since the surfaces act as efficient sinks. Loops with $\mathbf{b} = <100>$ which reach visible size become sessile, whereas $\mathbf{b} = \frac{1}{2}<111>$ loops remain mobile. Both types continue to grow by absorbing mobile submicroscopic clusters and smaller loops, and by coalescing with loops of comparable size. In the case of the mobile $\frac{1}{2}<111>$ loops, elastic interactions play an important role in this process. The relative proportions of the two loop types are probably determined by by a combination of factors, including their stabilities at small sizes, and the increased mobility of $\frac{1}{2}<111>$ loops at higher temperatures. At temperatures above 450°C, small $\frac{1}{2}<111>$ loops are less likely to form, and those which do are quickly subsumed into $<100>$ loops and never reach large sizes. At temperatures higher than 500°C this process may occur before any microscopic $\frac{1}{2}<111>$ loops form at all, and so such loops are not seen in the high temperature regime.

A final question concerns the fate of vacancies in our experiments. We have determined the nature of larger loops using the inside-outside contrast technique, and all were found to be interstitial. Evidence presented in this paper shows that most if not all of the mobile $\frac{1}{2}<111>$ loops are also interstitial in nature. Vacancy-rich regions are likely to form within cascades, but calculations suggest that closed vacancy loops of size ≤ 4nm are not formed, while small open loops transform to voids [22,23]. We have looked for but not found small voids in pure Fe, suggesting that any present are of size below the resolution limit of ~ 2nm. We did find very small voids in Fe8%Cr irradiated under similar conditions [5]. It is also possible that some of the small near-surface loops might be of vacancy nature [3].

### 5. Summary and conclusions

- We have described a transition in the microstructures of pure Fe produced by heavy-ion irradiation of thin foils which took place between irradiation temperatures $T_{irr}$ of 300°C and 500°C.

- Our previous work had shown that for ≤ 300°C, the microstructure was dominated by interstitial loops with Burgers vectors $\mathbf{b} = \frac{1}{2}<111>$. At $T_{irr} = 400$°C, about 50% of self-interstitials were still contained in $\frac{1}{2}<111>$ loops, which were frequently round or of irregular shape and had shear components. These loops were very mobile and frequently coalesced into larger loops. A high proportion of small, sessile, edge $<100>$ loops was also present, also accommodating about 50% of the interstitials.

- There was a gradual transition in microstructure at temperatures greater than 400°C. At $T_{irr} = 450$°C, loops with $\mathbf{b} = \frac{1}{2}<111>$ were still present, and interacted elastically to form long chains, but loops with $\mathbf{b} = <100>$ of pure edge character and rectilinear shape, now dominated in most areas, and accommodated a majority of the interstitials.

**Deleted:** a
**Deleted:** a/2
**Deleted:** a/2
**Deleted:** a/2
**Deleted:** a
**Deleted:** s
**Deleted:** a/2
**Deleted:** a/2
**Deleted:** a/2
**Deleted:**
**Deleted:** a/2
**Deleted:** a
**Deleted:** a/2

9

- At temperatures $T_{irr} \geq 450^{\circ}C$, small, mobile $\frac{1}{2}<111>$ loops were seen to be subsumed by sessile $<100>$ loops, and large $\frac{1}{2}<111>$ loops did not form. At $500^{\circ}C$, $<100>$ loops developed into large networks, and no visible $\frac{1}{2}<111>$ loops formed.

  | **Deleted:** a/2 |
  | **Deleted:** a/2 |
  | **Deleted:** a/2 |

- A plausible explanation of these observations has been given in terms of the relative stabilities of $\frac{1}{2}<111>$ and $<100>$ loops as a function of temperature, and the possible mechanism by which the microstructure develops.

  | **Deleted:** a/2 |
  | **Deleted:** a |

**References**

1. S. P. Fitzgerald and S. L. Dudarev, Proc. R. Soc. **A 464** 2549 (2008).
2. S. L. Dudarev, R. Bullough and P. M. Derlet, Phy. Rev. Lett., **100** 135503 (2008).
3. Z.Yao, M. Hernandez-Mayoral, M. L. Jenkins and M.A. Kirk, Phil. Mag. **88** 2851 (2008).
4. M. Hernandez-Mayoral, Z. Yao, M. L. Jenkins and M.A.Kirk, Phil. Mag. **88** 2881 (2008).
5. M. L. Jenkins, Z. Yao, M. Hernandez-Mayoral and M. A. Kirk, J. Nucl. Mat. **389** 5 (2009).
6. D. J. H. Cockayne, I. L. F.Ray and M. J. Whelan, Phil. Mag, **20** 1265 (1969).
7. M. L. Jenkins and M. A. Kirk (2001), Characterisation of Radiation Damage by Transmission Electron Microscopy, Institute of Physics Series in Microscopy in Materials Science (Series Editors, B Cantor and M J Goringe) ISBN 0 7503 0748 X (hbk)
8. K. Arakawa, K. Ono, M. Isshiki, K. Mimura, M. Uchikoshi and H. Mori, Science p.956, 318 (2007)
9. S. Fitzgerald and Z. Yao, Phil. Mag. Lett. (2009), in press.
10. Z. Zhou, M. L. Jenkins, S.L. Dudarev, A. Sutton and M. A. Kirk, Phil. Mag **86** 4851 (2006).
11. C. A. English and M. L. Jenkins, Phil. Mag. (2009), in press.
12. B. C. Masters, Phil. Mag. **11** 881 (1965).
13. Y. Konobeev, A. Dvoriashin, S. Porollo and F. Garner, J. Nucl. Mat. **355** 9 (2005).
14. D. Gelles, J Nucl. Mat. **108-9** 515 (1982).
15. S. Xu, Z. Yao and M.L. Jenkins, J. Nucl.Mat. (2009) in press.
16. B. L. Eyre and A. F. Bartlett, Phil. Mag. **12** 261 (1965).
17. M. L. Jenkins, C. A. English and B. L. Eyre, Phil. Mag. **38** 97 (1978).

10

18. M. A. Kirk., I. M. Robertson, M. L. Jenkins, C. A. English, T. J. Black and J. S. Vetrano,  J. Nucl. Mat. **149** 21 (1987).
19. K. Arakawa, M. Hatanaka, E. Kuramoto, K. Ono, and H. Mori, PRL **96** 125506 (2006)
20.  J. A. Turnbull, Phil. Mag. **21** 83 (1970).
21. D. J. Bacon, F. Gao and  Y. Osetsky, J. Nucl. Mat.  **276** (2000).
22. M. R. Gilbert, S. L. Dudarev, P. M. Derlet and D. G. Pettifor, J. Phys: Condens. Matter 20 345214 (2008).
23. M. R. Gilbert, Z. Yao, M. L. Jenkins and S. L. Dudarev, J. Nucl. Mat. **386-8** 36 (2009).

11

**Figure captions**

Figure 1:    Frames captured from video 2, showing loop coalescence in UHP Fe after irradiation at $400^oC$ to $1 \times 10^{18}$ ions m$^{-2}$. This occurred soon after ion irradiation ceased, as the specimen was being examined in the TEM and was still at $400^oC$. Three small $\frac{1}{2}$<111> loops towards the centre of frame A coalesce into a single $\frac{1}{2}$<111> loop in frame B. The loop is seen to rotate to new habit plane, frame C, and continues to hop.

Figure 2:    Contrast experiment at T$_{irr}$ = $400^oC$ in UHP Fe irradiated to a dose of $2 \times 10^{18}$ ions m$^{-2}$ (~1.3 dpa):(a) diffraction vector **g** = 020, so loops with **b** = [100] are out of contrast; (b) **g** = $01\bar{1}$ so loops with **b** = $\frac{1}{2}[\bar{1}11]$ and **b** = $\frac{1}{2}[111]$ are out of contrast; (c)  **g** = $00\bar{2}$ , so loops with **b** = [010] are out of contrast;(d) **g** = $0\bar{1}\bar{1}$ , so loops with **b** = $\frac{1}{2}[1\bar{1}1]$ and **b** = $\frac{1}{2}[11\bar{1}]$ are out of contrast.

Chains of $\frac{1}{2}$<111> loops are present together with a few large [001] loops and a large number of small loops of both types. In this field of view <001> loops outnumber $\frac{1}{2}$<111> loops about in a ratio of about 2:1.

Figure 3:    Experiment to determine the habit plane of $\frac{1}{2}[\bar{1}11]$ loops: (a) the specimen shown in figure 3 has been tilted close to the [310] pole. Loops with **b** = $\frac{1}{2}[\bar{1}11]$ appear edge-on on, consistent with a ($\bar{1}32$) habit plane ; (b) and (c) show experimental images of a two loops with  **b** = $\frac{1}{2}[\bar{1}11]$ at the [110] and [310] poles respectively.  TEMACI image simulations for a circular loop with this Burgers vector lying on ($\bar{1}32$) are inset at the lower left in each case.

Figure 4:    Loops in UHP Fe at $450^oC$ at a dose of 3 x $10^{18}$ ions m$^{-2}$: (a) long lines of large $\frac{1}{2}$<111> loops in a grain oriented about $20^o$ from [111]; (b) large loops of both types in an adjacent grain oriented close to [001], with <100> loops in a preponderance; (c) edge-on <100> loops in the same grain.

Figure 5    Formation of <100> loops in an [001] foil  at $500^oC$: (a) at a dose of $3 \times 10^{18}$ ions m$^{-2}$ (b) the same area at a dose of  1 x $10^{19}$ ions m$^{-2}$.

Figure 6    Stills extracted from video 6, showing single crystal [110] Fe under irradiation  at $465^oC$.  The large loop at the centre of the micrograph with **b** = <100> subsumes two smaller $\frac{1}{2}$<111> loops.

Figure 7:    Estimates of the fraction of interstitials contained in loops of the two types. The error bars do not take account of systematic errors due to loss of $\frac{1}{2}$<111> loops to the surface.

12

**List of videos**

Video 1    Early-stage damage development in UHP Fe irradiated at 400$^\circ$C. Viewed
           at 2 × real-time.

Video 2    Coalescence of three ½<111> loops at 400$^\circ$C under electron irradiation.
           Viewed in real-time.

Video 3    Elastic interaction of ½<111> loops to form loop chains at 400$^\circ$C under
           ion irradiation. Viewed at 30 × real-time.

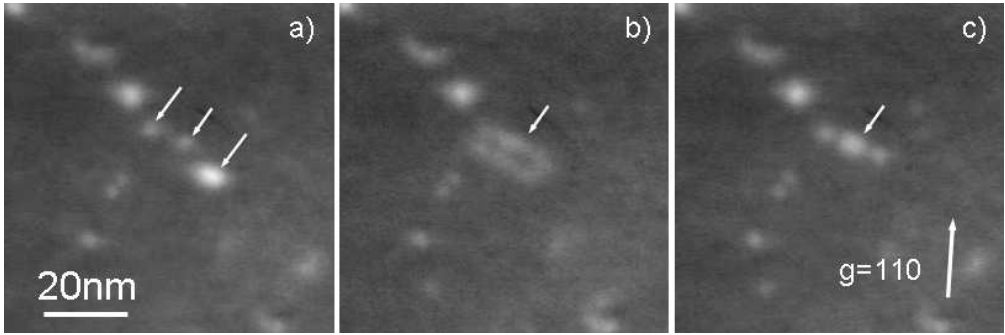Video 4    A tilt series reconstruction, showing large loops lie close to the foil centre.

Video 5    Loss of large [001] loops under ion irradiation in an [001] foil at 500$^\circ$C.
           Viewed at 10 × real-time.

Video 6    A large <100> loop subsumes two small ½<111> loops under ion
           irradiation at 465$^\circ$C. Viewed at 2 × real-time.

**Deleted:** a/2

**Deleted:** a/2

**Deleted:** a

**Deleted:** a

**Deleted:** a/2

13
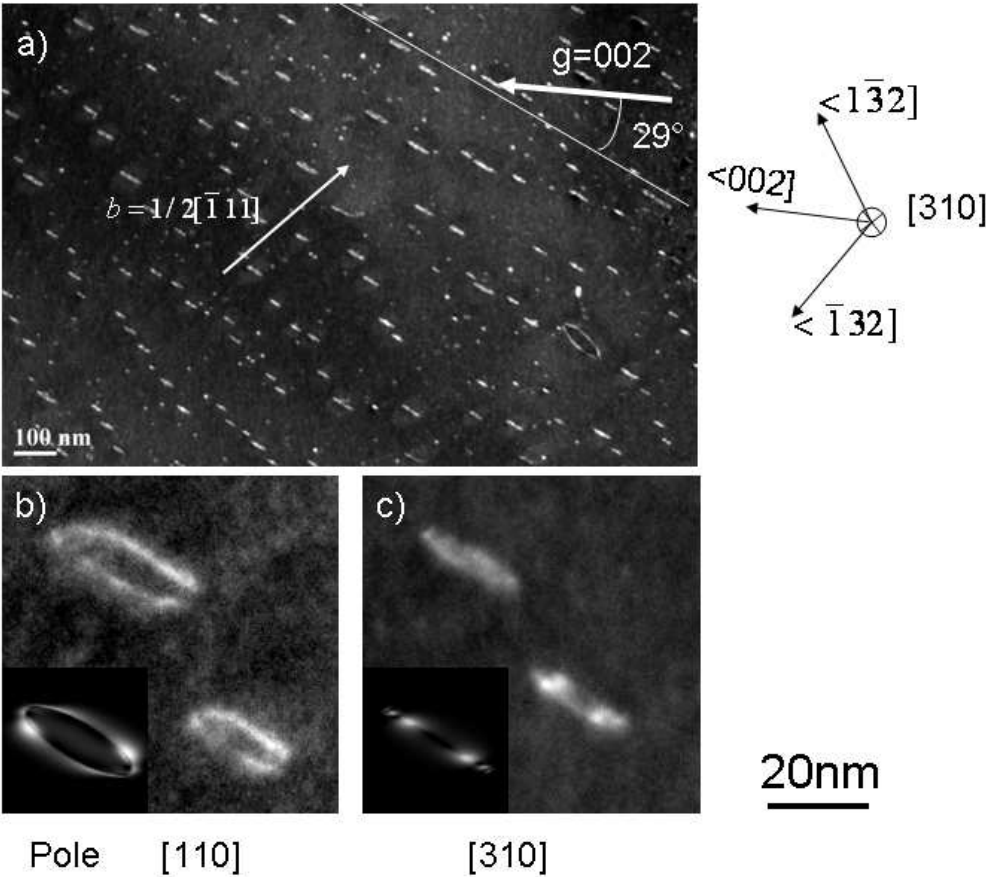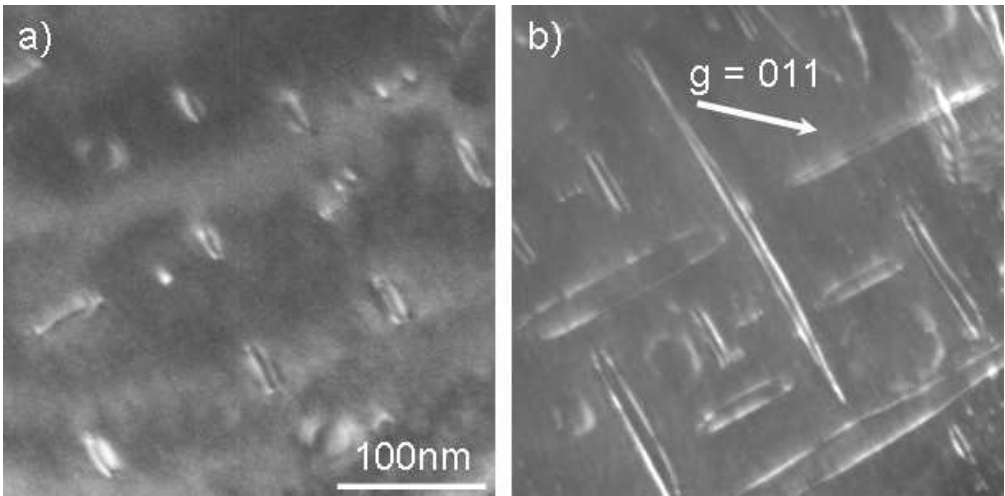
286x94mm (72 x 72 DPI)
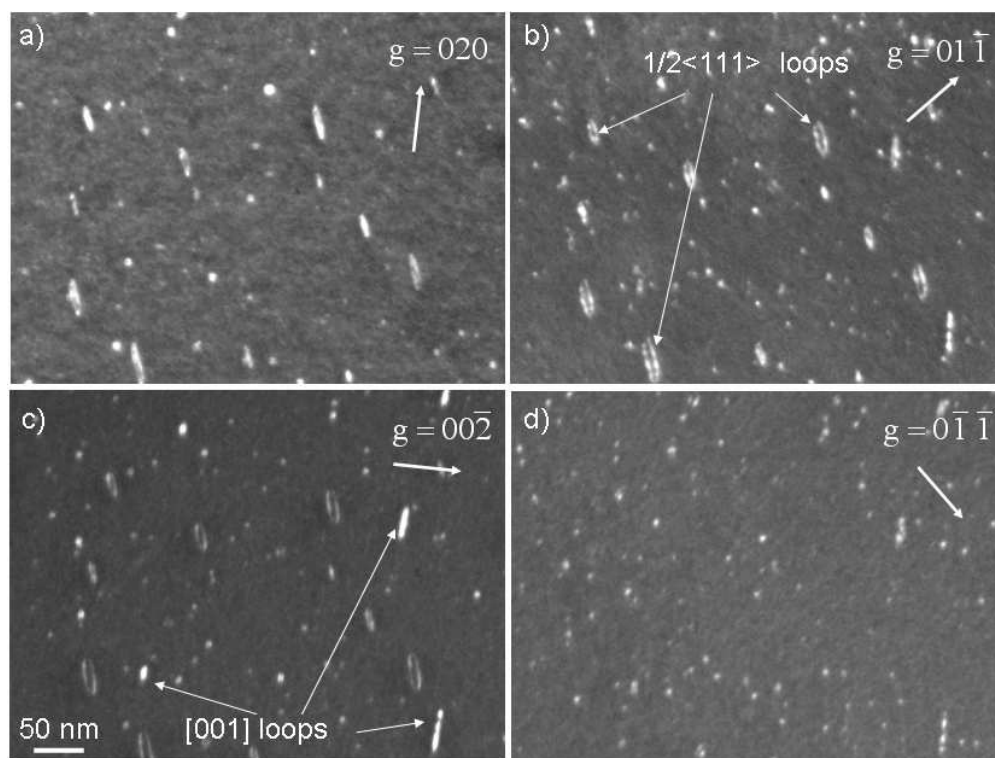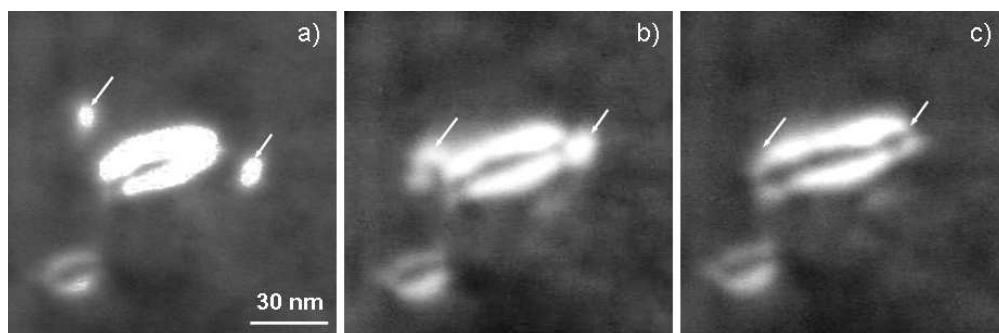
292x220mm (72 x 72 DPI)
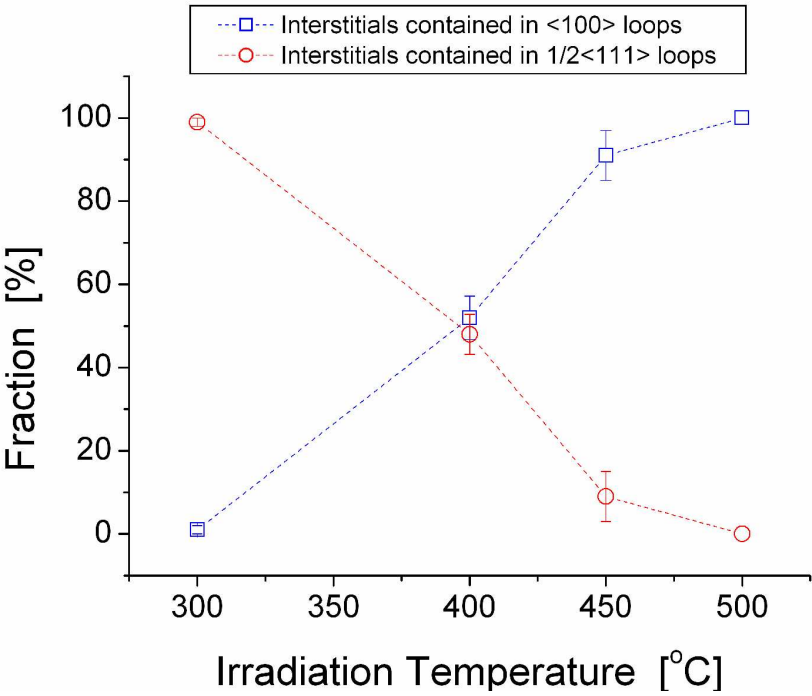
237x209mm (72 x 72 DPI)
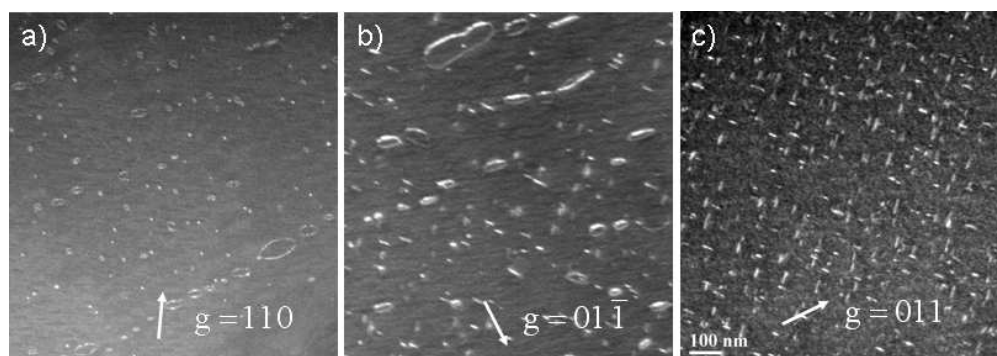
286x100mm (72 x 72 DPI)

215x105mm (72 x 72 DPI)

325x106mm (72 x 72 DPI)

575x399mm (150 x 150 DPI)